QUEEN'S UNIVERSITY BELFAST

How challenging is it to design a practical superdirective antenna array?

Asimonis, S. (2023). How challenging is it to design a practical superdirective antenna array? In *IEEE Sensors 2023: conference proceedings* (IEEE Sensors). Institute of Electrical and Electronics Engineers Inc.. https://doi.org/10.1109/SENSORS56945.2023.10325299

Published in:
IEEE Sensors 2023: conference proceedings

Document Version:
Publisher's PDF, also known as Version of record

Queen's University Belfast - Research Portal:
Link to publication record in Queen's University Belfast Research Portal

Publisher rights
© 2023 IEEE.
This work is made available online in accordance with the publisher's policies. Please refer to any applicable terms of use of the publisher.

General rights
Copyright for the publications made accessible via the Queen's University Belfast Research Portal is retained by the author(s) and / or other copyright owners and it is a condition of accessing these publications that users recognise and abide by the legal requirements associated with these rights.

Take down policy
The Research Portal is Queen's institutional repository that provides access to Queen's research output. Every effort has been made to ensure that content in the Research Portal does not infringe any person's rights, or applicable UK laws. If you discover content in the Research Portal that you believe breaches copyright or violates any law, please contact openaccess@qub.ac.uk.

Open Access
This research has been made openly available by Queen's academics and its Open Research team. We would love to hear how access to this research benefits you. – Share your feedback with us: http://go.qub.ac.uk/oa-feedback

Download date:19. Jul. 2024

How Challenging is it to Design a Practical Superdirective Antenna Array?

Stylianos D. Assimonis
Centre for Wireless Innovation (CWI), Institute of Electronics Communications and Information Technology (ECIT)
Queen's University Belfast
Belfast BT3 9DT, U.K.
s.assimonis@qub.ac.uk

***Abstract*—This work introduces the concept of the loaded dipole antenna array configuration in the design of low-complexity, easily implemented, and highly radiation-efficient superdirective antennas. Based on this concept, the design focuses on optimizing the loads rather than the input voltages, significantly simplifying the design process without the need for power amplifiers, attenuators, and phase shifters. A comprehensive theoretical analysis is presented and validated through numerical simulations, demonstrating excellent agreement between the analytical and numerical results.**

***Index Terms*—Antennas, Antenna arrays, Directive antennas, Superdirective antenna arrays**

I. Introduction

A superdirective antenna is characterized by an intensely focused radiation pattern, featuring a narrow main lobe in a particular direction. This type of antenna achieves higher directivity compared to a conventional antenna of similar size. Achieving superdirectivity involves closely spacing antenna elements, resulting in strong electromagnetic coupling. Noteworthy research by Uskov and others has explored superdirective antenna capabilities [1]–[9]. Studies show that a linear array with N isotropic elements can attain N^2+2N directivity as inter-element distance decreases. This level of superdirectivity surpasses uniform arrays with the same elements [10], [11]. Superdirective arrays radiate mainly perpendicular to the elements, forming end-fire antennas. However, practical superdirective antenna implementation faces challenges. High ohmic losses lead to lower efficiency and gain, affecting signal transmission. Achieving superdirectivity often demands intricate adjustments to element voltages using power amplifiers, attenuators, and phase shifters, adding complexity.

This work prioritizes antenna array gain maximization over directivity to address ohmic losses. In high contrast to the state-of-the-art, we employ a loaded dipole configuration, driving one dipole while loading others. This simplifies the design by focusing solely on optimizing loads, rather than input voltages. We extensively analyze a two-dipole array (extending to linear arrays) theoretically and through simulations, demonstrating strong agreement between analytical and numerical outcomes, reinforcing our approach's validity.

II. Antenna Design

Fig. 1 shows two antenna dipoles placed side-by-side at distance d, each being a half-wavelength wire ($L_1 = L_2 = \lambda/2$) with radii a_1 and a_2. Operating at 3.5 GHz (sub-6 GHz 5G), the dipoles' proximity results in mutual coupling, allowing modelling as a two-port network. Port 1 and port 2 feature input voltages and currents v_1, v_2, and i_1, i_2, respectively. The system behaviour employs Z-parameters for mathematical characterization, which are defined as follows:

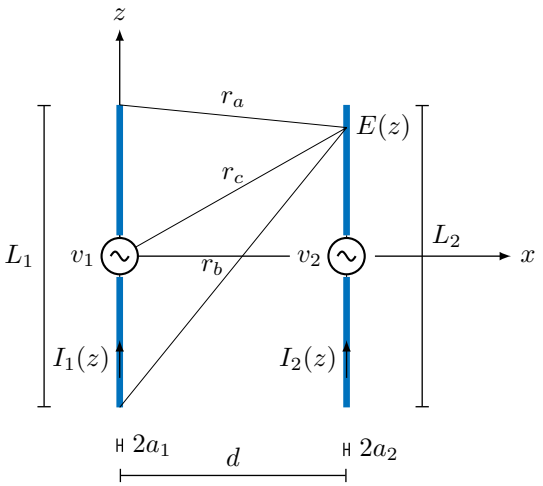

Fig. 1. A configuration of wire dipole antennas is formed, with elements of lengths L_1 and L_2, radii a_1 and a_2, and an inter-element distance of d.

$$\begin{bmatrix} v_1 \\ v_2 \end{bmatrix} = \begin{bmatrix} z_{11} & z_{12} \\ z_{21} & z_{22} \end{bmatrix} \begin{bmatrix} i_1 \\ i_2 \end{bmatrix} \tag{1}$$

In this context, z_{11} and z_{22} denote self-impedances of dipoles, while z_{12} and z_{21} represent mutual impedances that describe inter-dipole coupling. z_{11} and z_{22} are termed *open-circuit* input/output impedances, while z_{21} and z_{12} are forward/reverse transfer impedances, respectively. These names arise from these impedances being defined based on open-circuit voltage at ports 1 or 2. To estimate them, open-circuit voltage at ports must be determined, calculated by integrating electric field over dipoles. Assuming the first dipole is driven and second is open-circuited ($i_1 \neq 0$, $i_2 = 0$), open-circuit voltage at the second dipole is evaluated by integrating the field from the first dipole. This is mathematically expressed

as [12]:

$$V_2^{oc} = -\frac{1}{i_2}\int_{-\frac{L_2}{2}}^{\frac{L_2}{2}} E\left(z\right) I_2\left(z\right)\,\mathrm{d}z, \tag{2}$$

where $E\left(z\right)$ represents the electric field component parallel to dipole 2, generated by the first driven dipole, and $I_2\left(z\right)$ represents the resulting current distribution along the second dipole. Please note that $E\left(z\right)$ and $I_2\left(z\right)$ are functions that need to be estimated.

As for the current distribution, we make the assumption that it follows a sinusoidal pattern, which can be expressed as:

$$I_2\left(z\right) = i_2 \frac{\sin\left(k\left(\frac{L_2}{2} - |z|\right)\right)}{\sin\left(\frac{k\,L_2}{2}\right)}, \tag{3}$$

where, $k = 2\pi/\lambda$ is the wavenumber, and λ is the wavelength. This assumption holds true when the radius of the dipoles is relatively small. In this case, we consider $a_1 = a_2 = \lambda/1001$ for the dipoles' radius.

The electric field generated by the driven dipole 1, acting on dipole 2, can be represented as:

$$\begin{aligned} E_z\left(z\right) = -j\frac{\eta_0 i_1}{4\pi\sin\left(\frac{k\,L_1}{2}\right)}\Bigg\{&\frac{e^{-jkr_a}}{r_a} + \frac{e^{-jkr_b}}{r_b} \\ &- 2\cos\left[\frac{k\,L_1}{2}\right]\frac{e^{-jkr_c}}{r_c}\Bigg\}, \end{aligned} \tag{4}$$

where η_0 is the characteristic impedance of free space and

$$\begin{aligned} &r_a = \sqrt{d^2 + \left(z - L_1/2\right)^2} \quad r_b = \sqrt{d^2 + \left(z + L_1/2\right)^2} \\ &r_c = \sqrt{d^2 + z^2}. \end{aligned} \tag{5}$$

Based on the definition of z_{21}:

$$z_{21} \triangleq \left.\frac{v_2}{i_1}\right|_{i_2=0} = \frac{V_2^{oc}}{i_1} \tag{6}$$

and thus,

$$\begin{aligned} z_{21} = j\frac{\eta_0}{4\pi\sin\left(\frac{k\,l_1}{2}\right)\sin\left(\frac{k\,l_2}{2}\right)}\int_{-\frac{L_2}{2}}^{\frac{L_2}{2}}\Bigg\{&\frac{e^{-jkr_a}}{r_a} + \frac{e^{-jkr_b}}{r_b} \\ &- 2\cos\left[\frac{k\,L_1}{2}\right]\frac{e^{-jkr_c}}{r_c}\Bigg\}\sin\left[k\left(\frac{L_2}{2} - |z|\right)\right]\mathrm{d}z \end{aligned} \tag{7}$$

It is important to note that the integral in (7) does not have an analytical solution. Therefore, we employed numerical integration techniques, specifically global adaptive quadrature, to precisely evaluate the integral [13]. Also, according to reciprocity, $z_{21} = z_{12}$.

To estimate the self-impedance z_{11}, we can employ a similar analysis by evaluating the integral over the surface of the first dipole. Again, we assume a sinusoidal current distribution, resulting in the following expression:

$$\begin{aligned} z_{11} = j\frac{\eta_0}{4\pi\sin^2\left(\frac{k\,l_1}{2}\right)}\int_{-\frac{l_1}{2}}^{\frac{l_1}{2}}\Bigg\{&\frac{e^{-jkr_a}}{r_a} + \frac{e^{-jkr_b}}{r_b} \\ &- 2\cos\left[\frac{k\,L_1}{2}\right]\frac{e^{-jkr_c}}{r_c}\Bigg\}\sin\left[k\left(\frac{L_1}{2} - |z|\right)\right]\mathrm{d}z \end{aligned} \tag{8}$$

and now

$$\begin{aligned} &r_a = \sqrt{a_1^2 + \left(z - L_1/2\right)^2} \quad r_b = \sqrt{a_1^2 + \left(z + L_1/2\right)^2} \\ &r_c = \sqrt{a_1^2 + z^2}. \end{aligned} \tag{9}$$

Similar analysis can be applied to estimate z_{22}.

Assuming that the dipoles are driven by the input voltages v_1 and v_2, we can estimate the Z-parameters through (7) and (8), enabling us to solve (1) for the corresponding input currents, i_1 and i_2. Subsequently, classical antenna theory can be applied to estimate the directivity of the antenna array. Specifically, the radiation intensity of the antenna array can be expressed as follows:

$$U\left(\theta,\phi\right) = \frac{\eta_0}{8\,\pi^2}\left|\sum_{n=1}^{2} i_n f_n e^{j\vec{k}\cdot\vec{d_i}}\right|^2 \tag{10}$$

where

$$f_n = \frac{\cos\left(\frac{k\,L_n}{2}\cos\theta\right) - \cos\left(\frac{k\,L_n}{2}\right)}{\sin\left(\frac{k\,L_n}{2}\right)\sin\theta} \tag{11}$$

is the radiation pattern of each dipole, and $\vec{k} = k\hat{r}$ is the wavevector, where

$$\hat{r} = \sin\theta\cos\phi\,\hat{x} + \sin\theta\sin\phi\,\hat{y} + \cos\theta\,\hat{z}, \tag{12}$$

is the unit vector in spherical coordinates, and $\vec{d_i} = x_i,\hat{x} + y_i,\hat{y} + z_i,\hat{z}$ is the vector that indicates the position of the dipoles.

The directivity of the antenna array is defined as

$$D \triangleq 4\pi\frac{U\left(\theta,\phi\right)}{P_r}, \tag{13}$$

where

$$P_r \triangleq \int_{\phi=0}^{2\pi}\int_{\theta=0}^{\pi} U\left(\theta,\phi\right)\sin\theta\,\mathrm{d}\theta\mathrm{d}\phi, \tag{14}$$

is the total radiated power.

The gain of the antenna array is defined as:

$$G \triangleq 4\pi\frac{U\left(\theta,\phi\right)}{P_{in}}. \tag{15}$$

where, P_{in} is the input power to the antenna system and it is given by:

$$P_{in} \triangleq P_r + P_l, \tag{16}$$

where P_l represents the ohmic losses on the dipoles. The presence of Ohmic losses is attributed to the *skin effect* [14]. By considering this effect, we can determine the loss resistance per unit length on the i-th conductive wire dipole as follows:

$$r_l^{(n)} = \frac{1}{2a_i}\sqrt{\frac{f\mu_0}{\pi\sigma}}, \tag{17}$$

here f, $\mu_0 = 4\pi\times10^{-7}$ H/m, and σ represent the operating frequency, magnetic permeability of free space, and wire conductivity, respectively. Therefore, for the current distribution given by (3)

$$R_l^{(n)} = r_l^{(n)}\int_{-\frac{L_n}{2}}^{\frac{L_n}{2}}\left|\frac{I_n\left(z\right)}{i_n}\right|^2\mathrm{d}z = \frac{kL_i - \sin\left(kL_i\right)}{4ka_i\sin^2\left(k\frac{L_i}{2}\right)}\sqrt{\frac{f\mu_0}{\pi\sigma}}. \tag{18}$$

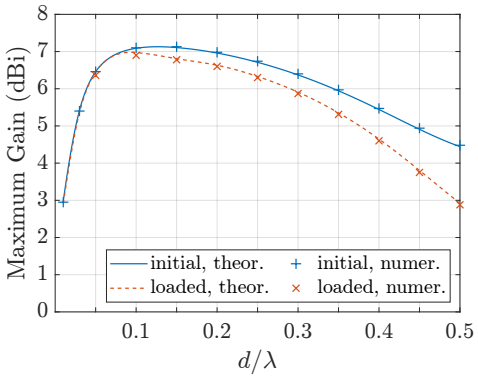

Fig. 2. The maximum end-fire gain of the antenna array (in dBi) is plotted against the inter-element distance. Initially, the antenna array was optimized using the input voltages v_1 and v_2 as design parameters, resulting in four parameters considering the complex nature of the voltages. In the subsequent case (*loaded*-case), only the first dipole was driven by a voltage of $v_1 = 1$ V (rms value), while the second dipole was loaded with an impedance of Z_l, making the load Z_l the sole design parameter. The analytical results were validated through numerical simulations using 4nec2. A very good agreement is observed. Also, the results reveal that for $d = 0.1\lambda$, there is no need to use any power amplifier, attenuator, or phase shifter to achieve superdirectivity, but only a load of $Z_l = -j54.11\ \Omega$ connected to the second dipole.

Hence, (1) is now expressed as

$$\begin{bmatrix} v_1 \\ v_2 \end{bmatrix} = \begin{bmatrix} z_{11} + R_l^{(1)} & z_{12} \\ z_{21} & z_{22} + R_l^{(2)} \end{bmatrix} \begin{bmatrix} i_1 \\ i_2 \end{bmatrix}. \tag{19}$$

and to calculate the gain, it is necessary to solve this system for the currents.

Our goal is to create an antenna array achieving superdirectivity. Particle Swarm Optimization (PSO) was used for optimization to find the maximum gain G as a function of the interelement distance. Firstly, the design parameters considered were the input voltages v_1 and v_2. Superdirective antenna arrays have a well-known end-fire pattern directed perpendicular to the elements. The gain was evaluated at $(\theta, \phi) = (\pi/2, 0)$ and $(\theta, \phi) = (\pi/2, \pi)$, representing the $\pm x$-axis, as illustrated in Fig. 2. The maximum gain of 7.1 dBi occurs at $d = 0.1\lambda$. Reducing d lowers the gain due to increased mutual coupling (z_{21}, z_{12}), which leads to intensified input currents and distribution. Consequently, this results in higher ohmic losses.

Next, in order to simplify the design complexity, we make the assumption that the first dipole is driven by a voltage $v_1 = 1$ V (rms value), while the second dipole is loaded with an impedance Z_l. Consequently, the equivalent circuit of this antenna array is illustrated in Fig. 3. With this configuration, the system representing the two-port network in Fig. 3 is expressed as follows:

$$\begin{bmatrix} v_1 \\ 0 \end{bmatrix} = \begin{bmatrix} z_{11} + R_l^{(1)} & z_{12} \\ z_{21} & z_{22} + R_l^{(2)} + Z_l \end{bmatrix} \begin{bmatrix} i_1 \\ i_2 \end{bmatrix} \tag{20}$$

and in order to calculate the gain, this system must be solved for the currents.

Once again, PSO was employed to determine the maximum gain (G) versus inter-element distance. This time, the design

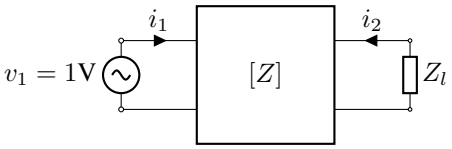

Fig. 3. The first dipole is driven by the voltage v_1, while the second dipole is loaded with the impedance Z_l. This particular configuration greatly simplifies the design complexity of the antenna array, allowing us to achieve superdirectivity without the need for power amplifiers, attenuators, or phase shifters.

parameter used was solely the load Z_l, significantly reducing the design complexity as there is no need for power amplifiers, attenuators, or phase shifters. The optimization results are presented in Fig. 2. It is evident that for an inter-element distance of 0.1λ, the maximum end-fire gain is 6.9 dBi, which is very close to the corresponding gain achieved when optimizing v_1 and v_2, i.e., four design parameters (complex voltages v_1 and v_2). Additionally, the optimal load is $Z_l = -j54.11$ Ω, indicating a purely capacitive load. This finding is highly promising as it demonstrates that the design of a superdirective antenna array is achievable by driving a single element and loading the other element with a capacitive load.

In order to validate our theoretical results, we utilized 4nec2 [15], a widely-used software tool for modelling and simulating antenna systems. 4nec2 employs the method of moments (MoM) as a numerical electromagnetic field solver to analyze and predict antenna behavior. The results obtained from 4nec2 are depicted in Fig. 2, which includes the cases where both voltages v_1 and v_2 were optimized to achieve maximum end-fire gain (initial), as well as the case where only the load Z_l was optimized (loaded). A very good agreement is observed.

III. Conclusions

This study demonstrates that creating a high-efficiency superdirective antenna is less challenging than previously believed. By employing a loaded dipole configuration, focusing on optimal load values instead of input voltages, the design process is streamlined. This approach simplifies the complexity of designing superdirective antenna arrays, eliminating the need for power amplifiers, attenuators, and phase shifters. Through a thorough analysis of a two-dipole antenna array, our approach's effectiveness is showcased, extensible to linear arrays. Numerical simulations confirm analytical accuracy, endorsing our method. This research aids the development of practical, efficient superdirective antenna arrays with simplified designs. With its superdirective characteristics and high gain, this antenna design offers substantial potential for sensing applications. The focused, directional radiation pattern allows precise targeting and sensing of specific regions or objects of interest. Its simplified design process renders it compatible for integration into diverse sensing devices and platforms, such as wireless sensor networks, radar systems, and remote sensing applications. Additionally, the heightened radiation efficiency positions this antenna as an ideal contender for wireless power transfer applications.

REFERENCES

[1] A. I. Uzkov, "An approach to the problem of optimum directive antenna design," *Comptes Rendus (Doklady) de l'Academie des Sciences de l'URSS*, vol. 53, p. 35–38, 1946.

[2] R. Harrington, "On the gain and beamwidth of directional antennas," *IRE Transactions on Antennas and Propagation*, vol. 6, no. 3, pp. 219–225, 1958.

[3] ——, "Antenna excitation for maximum gain," *IEEE Transactions on Antennas and Propagation*, vol. 13, no. 6, pp. 896–903, 1965.

[4] A. D. Yaghjian, T. H. O'Donnell, E. E. Altshuler, and S. R. Best, "Electrically small supergain end-fire arrays," *Radio Science*, vol. 43, no. 03, pp. 1–13, 2008.

[5] A. M. H. Wong and G. V. Eleftheriades, "Adaptation of schelkunoff's superdirective antenna theory for the realization of superoscillatory antenna arrays," *IEEE Antennas and Wireless Propagation Letters*, vol. 9, pp. 315–318, 2010.

[6] J. M. Lugo, J. de Almeida Goes, A. Louzir, P. Minard, D. Lo Hine Tong, and C. Person, "Design, optimization and characterization of a superdirective antenna array," in *2013 7th European Conference on Antennas and Propagation (EuCAP)*, 2013, pp. 3736–3739.

[7] K. Dovelos, S. D. Assimonis, H. Q. Ngo, and M. Matthaiou, "Superdirective arrays with finite-length dipoles: Modeling and new perspectives," in *GLOBECOM 2022 - 2022 IEEE Global Communications Conference*, 2022, pp. 6517–6522.

[8] E. Altshuler, T. O'Donnell, A. Yaghjian, and S. Best, "A monopole superdirective array," *IEEE Transactions on Antennas and Propagation*, vol. 53, no. 8, pp. 2653–2661, 2005.

[9] K. Dovelos, S. D. Assimonis, H. Q. Ngo, and M. Matthaiou, "Superdirective antenna pairs for energy-efficient terahertz massive mimo," *arXiv preprint arXiv:2207.00697*, 2022. [Online]. Available: https://arxiv.org/abs/2207.00697

[10] S. D. Assimonis, T. Samaras, and V. Fusco, "Analysis of the microstrip-grid array antenna and proposal of a new high-gain, low-complexity and planar long-range wifi antenna," *IET Microwaves, Antennas & Propagation*, vol. 12, no. 3, pp. 332–338, 2018. [Online]. Available: https://ietresearch.onlinelibrary.wiley.com/doi/abs/10.1049/iet-map.2017.0548

[11] S. D. Assimonis, M. A. B. Abbasi, and V. Fusco, "Millimeter-wave multi-mode circular antenna array for uni-cast multi-cast and oam communication," *Scientific Reports*, vol. 11, no. 1, p. 4928, Mar 2021. [Online]. Available: https://doi.org/10.1038/s41598-021-83301-1

[12] S. J. Orfanidis. (2016) Electromagnetic waves and antennas. [Online]. Available: http://eceweb1.rutgers.edu/ orfanidi/ewa/

[13] L. F. Shampine, "Vectorized adaptive quadrature in MATLAB," *Journal of Computational and Applied Mathematics*, vol. 211, pp. 131–140, 2008.

[14] C. A. Balanis, *Antenna theory: Analysis and Design*. John Wiley & Sons, 2005.

[15] "4nec2 software," Available online, Year. [Online]. Available: https://www.qsl.net/4nec2/